Novel views on endotyping asthma, its remission, and COPD

Carpaij, Orestes

DOI:
10.33612/diss.136744640

Chapter 9

Optical coherence tomography intensity correlates with extra-cellular matrix components in the airway wall

Orestes A. Carpaij[#], Annika W.M. Goorsenberg[#], Julia N.S. d'Hooghe, D. Martijn de Bruin, Richard M. van den Elzen, Martijn C. Nawijn, Jouke T. Annema, Maarten van den Berge, Peter I. Bonta[*], Janette K. Burgess[*]

#: shared first author
*: shared last author

Am J Respir Crit Care Med. 2020 Apr 30

Introduction

Obstructive pulmonary diseases are characterised by structural airway remodeling, including alterations in the extracellular matrix (ECM) [1]. Studies have shown that the ECM profile differs in asthmatic airways compared to non-asthmatics, with less elastin, and higher abundance of collagen I and fibronectin in asthma [2]. Additionally, increased airway wall collagen deposition is associated with more severe disease in asthma [3]. In COPD, alterations in collagen and elastin affect the mechanical properties of the lung, subsequently decreasing the lung elasticity and contributing to emphysema [1]. Currently, two diagnostic tools are available to assess airway remodeling: (high resolution) computed tomography (HRCT) of the chest and immunohistochemistry in endobronchial biopsies. While bronchial wall thickness and lumen area can be assessed by HRCT, the resolution is not sufficient to assess separate airway wall layers and ECM components leaving the pathophysiology of airway wall remodeling unclear. Biopsies are the gold standard for determining airway remodeling; however, the applicability is limited due to its invasiveness, small sample area and elaborative histology processing.

Optical coherence tomography (OCT) generates high resolution, real-time, near-infrared-based cross-sectional images of the airway wall [4,5], with potential for visualizing airway remodeling and enabling three-dimensional airway wall reconstructions. Several studies found an increased airway wall thickness and decreased lumen area in asthma and COPD patients using OCT [5,6]. Furthermore, OCT imaging was able to identify and quantify mucosal and submucosal airway layers [4]. To the best of our knowledge, no study has linked OCT imaging to ECM protein deposition in the airway wall. We hypothesized that the ECM deposition within the airway wall can be detected using OCT. The aim of this study was to relate the OCT scattering characteristics with ECM deposition in the airway wall.

Methods

Data were acquired as previously described [4]. The local medical ethics committee approved the protocol (NL51605.018.14) and informed consent was obtained. In brief, five patients scheduled for a lobectomy were included. From these five lobectomy specimens, thirteen airways were dissected and marked with needles to match ex-vivo OCT images with 51 histological sections. Ex-vivo OCT imaging was performed immediately after resection, using a C7 Dragonfly catheter from St Jude Medical (St Paul, MN, USA). The OCT images were analysed using Matlab software (Natick MA, USA), which enabled roll-off correction and point spread function as previously described [7]. Three sequential frames were combined to minimize noise. Sheath and lumen segmentation was applied according to Adams *et al.* to minimize the influence of scattering intense components in the lumen [8]. OCT mm^2 areas were calculated using a threshold in light scattering intensity, illustrated in figure 1A. To correct for probe optics and the imperfect sampling of the OCT system in depth, the fixed threshold was adjusted for the distance between the lumen and the airway wall in each axial line: a lower threshold was used in larger distances as compared with a higher threshold in shorter distances. For each calculated OCT area, the median OCT intensity (arbitrary units) was measured.

The histological sections were stained with the following biochemical or antigen stainings: Picosirius Red (TC; total collagen), Masson's Trichrome blue (MT blue; total collagen and bone), anti-collagen A1 antibody (CA1; collagen type 1 A1), Verhoeff's (EL; elastin) and anti-fibronectin antibody (FN; fibronectin). The region of interest (ROI) was defined as the area of the airway wall between the epithelium and the outer border of the desmin-positive smooth muscle. Sections without distortions within the ROI were included. The stained sections for each airway were aligned and colour deconvoluted using ImageJ software [9]. Thereafter, the positive mm^2 area (threshold >150 of 255 max grayscale intensity) and the mean grayscale (0-255: lowest-highest intensity) of the stained airway wall were calculated. Correlations were calculated using the Spearman's rank correlation coefficient.

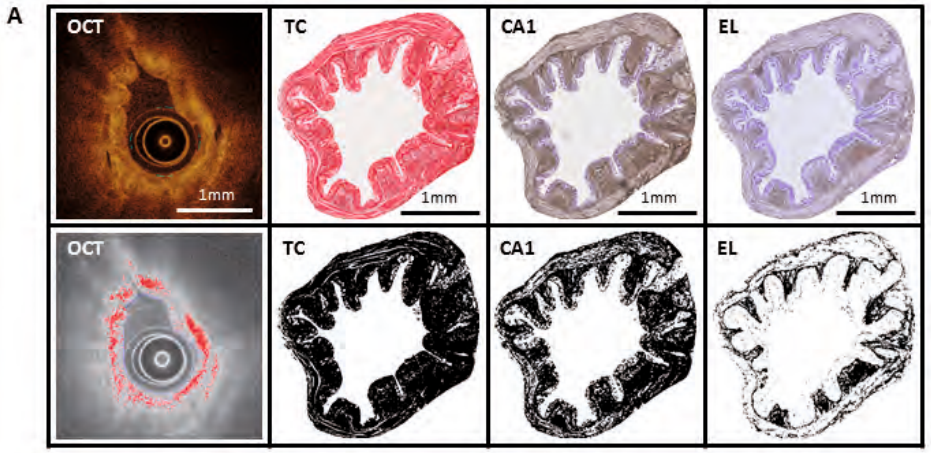

Figure 1: illustration of methods for correlating OCT image with ECM staining sections. **1A:** Three airway wall ECM staining sections aligned to the paired OCT-image, **OCT:** optical coherence tomography image with the area above the threshold (threshold per axial line for the distance between the lumen and the airway wall) in red, **TC:** total collagen, **CA1:** collagen A1, **EL:** elastin, all three stained sections with the area above the threshold (i.e. >150 of 255 grayscale) in black. **1B:** Spearman's correlation of OCT area with TC area in mm², CA1 area in mm² and EL area in mm² respectively. **1C:** Spearman's correlation of OCT intensity with TC mean grayscale, CA1 mean grayscale, and EL mean grayscale respectively.

Results and discussion

A total of 36 from the 51 OCT-histology pairs from the right upper lobe and left lower lobe were analysed. Reasons for exclusion were damaged histology sections (7 pairs), unavailability of histology for additional staining (2 pairs) and when the OCT image was taken at a bifurcation (2 pairs) (supplementary table 1). The mean lumen area of the included sections was 2.38 (±2.06) mm². ECM component stained areas showed a similar spatial pattern as the OCT threshold measured area (figure 1A). Quantification of ECM component stained areas in mm² were significantly positively correlated with the OCT area, while total collagen, MT blue, and collagen A1 mean grayscale correlated with OCT intensity as well (table 1).

Table 1: Spearman's correlations paired OCT-histology areas and intensities

	Optical Coherence Tomography Area (mm²)		Optical Coherence Tomography Intensity (arbitrary unit)	
	R-value	P-value	R-value	P-value
Total collagen area (mm²)	**0.554**	**<0.001**	-	-
Total collagen mean grayscale	-	-	**0.395**	**0.017**
Masson's Trichrome blue area (mm²)	**0.427**	**0.012**	-	-
Masson's Trichrome blue mean grayscale	-	-	**0.466**	**0.005**
Collagen A1 area (mm²)	**0.537**	**0.001**	-	-
Collagen A1 mean grayscale	-	-	**0.427**	**0.010**
Elastin area (mm²)	**0.639**	**<0.001**	-	-
Elastin mean grayscale	-	-	0.254	0.168
Fibronectin area (mm²)	**0.622**	**<0.001**	-	-
Fibronectin mean grayscale	-	-	0.138	0.468

This study shows for the first time that OCT is able to detect and quantify ECM protein deposition in the airway wall. In other research areas focusing on skin and ovarian tissue, an association has been made between collagen deposition and OCT imaging [10,11]. In the airways however, OCT imaging studies have mainly focused on the identification and quantification of the airway wall structure. Intriguingly, elastin and fibronectin area correlated the strongest with OCT area, yet no significance was found between intensity parameters. Further research is required to determine light scattering properties of these ECM components separately.

Our findings that OCT may directly reflect collagen deposition, without the need of extracting endobronchial biopsies, is of specific interest in obstructive lung diseases in which airway remodeling plays an important role. Furthermore, by assessing not only the thickness but also ECM content of the airway wall, it might be possible to monitor treatments targeting airway remodeling in more detail such as bronchial thermoplasty and liquid nitrogen spray.

An achievement of this study is the development of an automated analysis of the OCT image and light scattering intensity areas by threshold and segmentation technique. While in previous studies OCT areas were drawn manually, this study shows that by using a light scattering –based intensity threshold, it is possible to automatically identify and quantify ECM structures. Additionally, by combining this method with innovative polarization sensitive - OCT systems, it may be possible to identify and quantify individual structural components of the airway wall with even greater accuracy [12].

Several limitations need to be addressed. First, in order to make a comparison between OCT and histology we used ex-vivo material. However, by using this approach we were able to assess ECM structures of the entire airway wall in a cross sectional manner, while endobronchial in-vivo biopsies only give superficial mucosal information from one specific location in the airways. Second, we were not able to use all OCT images or histological sections due to damage or artifacts. Despite these, a strong correlation between OCT light scattering areas and ECM stained components within the airways was found.

Conclusion

In conclusion, our data shows that increased OCT intensity area locations correspond and correlate with higher collagen, elastin and fibronectin areas in the airway wall. This suggests that it is now possible to directly measure airway remodeling in vivo, in a minimally invasive, real-time manner.

Supplementary table 1: distribution of lung segments and excluded samples

	Segment	**Excluded in the present study**
Patient 1	RB3: 4 pairs	All (4 pairs): no histology available
Patient 2	LB7 anterior subsegment: 2 pairs	
	LB7 posterior subsegment: 2 pairs	All (2 pairs): OCT images taken on a bifurcation
	LB10: 1 pair	
Patient 3	LB10 left subsegment: 3 pairs	1 pair excluded: damaged histology
	LB10 right subsegment: 7 pairs	
Patient 4	LB8 right subsegment: 4 pairs	1 pair excluded: damaged histology
	LB9: 5 pairs	1 pair excluded: no histology available
	LB10: 6 pairs	2 pairs excluded: damaged histology
Patient 5	RB3: 6 pairs	1 pair excluded: damaged histology
	RB2: 3 pairs	1 pair excluded: damaged histology
	RB1 lateral subsegment: 4 pairs	
	RB1 medial subsegment: 4 pairs	2 pairs excluded: damaged histology

A

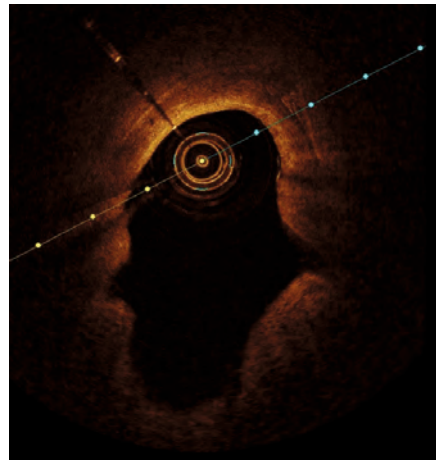

B

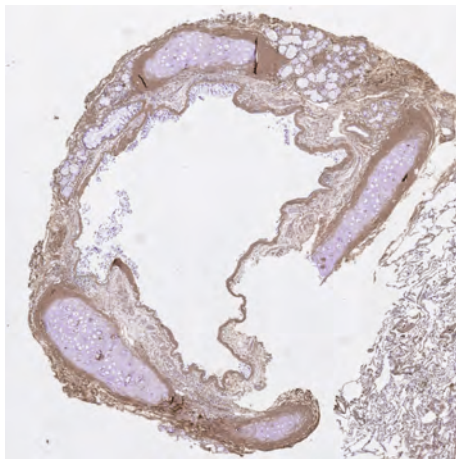

Supplementary figure 1: examples of excluded images and histological sections. **1A:** example of an excluded OCT image taken from a bifurcation, **1B:** example of an excluded damaged histological section.

References

1 Ito JT, Lourenço JD, Righetti RF, et al. Extracellular Matrix Component Remodeling in Respiratory Diseases: What Has Been Found in Clinical and Experimental Studies? Cells 2019;8:342.

2 Vignola AM, Kips J, Bousquet J. Tissue remodeling as a feature of persistent asthma. J Allergy Clin Immunol 2000;105:1041–53.

3 Benayoun L, Druilhe A, Dombret M-C, et al. Airway structural alterations selectively associated with severe asthma. Am J Respir Crit Care Med 2003;167:1360–8.

4 D'Hooghe JNS, Goorsenberg AWM, De Bruin DM, et al. Optical coherence tomography for identification and quantification of human airway wall layers. PLoS One 2017;12:1–13.

5 Ding M, Chen Y, Guan WJ, et al. Measuring Airway Remodeling in Patients With Different COPD Staging Using Endobronchial Optical Coherence Tomography. Chest 2016;150:1281–90.

6 Hariri LP, Adams DC, Applegate MB, et al. Distinguishing tumor from associated fibrosis to increase diagnostic biopsy yield with polarization-sensitive optical coherence tomography. Clin Cancer Res 2019;:clincanres.0566.2019.

7 Freund JE, Faber DJ, Bus MT, et al. Grading upper tract urothelial carcinoma with the attenuation coefficient of in-vivo optical coherence tomography. Lasers Surg Med 2019;51:399–406.

8 Adams DC, Pahlevaninezhad H, Szabari M V, et al. Automated segmentation and quantification of airway mucus with endobronchial optical coherence tomography. Biomed Opt Express 2017;8:4729–41.

9 Schneider CA, Rasband WS, Eliceiri KW. NIH Image to ImageJ: 25 years of image analysis. Nat Methods 2012;9:671–5.

10 Ud-Din S, Foden P, Stocking K, et al. Objective assessment of dermal fibrosis in cutaneous scarring: using optical coherence tomography, high frequency ultrasound and immuno-histo-morphometry of human skin. Br J Dermatol 2019;:0–2.

11 Yang Y, Wang T, Biswal NC, et al. Optical scattering coefficient estimated by optical coherence tomography correlates with collagen content in ovarian tissue. J Biomed Opt 2011;16:090504.

12 Feroldi F, Davidoui V, Gräfe M, et al. In vivo multifunctional optical coherence tomography at the periphery of the lungs. Biomed Opt Express. 2019 May 30;10(6):3070-3091.